 doi:10.20944/preprints202011.0660.v1

Article

Mechanical Characterization of Graphene Nanoplatelets-Reinforced Mg-3Sn Alloy Synthesized by Powder Metallurgy

Pravir Kumar [1], Katerina Skotnicova [2], Ashis Mallick [1], Manoj Gupta [3,*], Tomas Cegan [2] and Jan Jurica [2]

[1] Department of Mechanical Engineering, Indian Institute of Technology (ISM) Dhanbad Dhanbad – 826 004, India; pravirkumar30@gmail.com (P.K); mallick@iitism.ac.in (A.M)
[2] Faculty of Materials Science and Technology, VSB-Technical University of Ostrava, Ostrava-70800, Czech Republic; katerina.skotnicova@vsb.cz (K.S); tomas.cegan@vsb.cz (T.C); jan.jurica@vsb.cz (J.J)
[3] Department of Mechanical Engineering, National University of Singapore, Singapore–117576, Singapore; mpegm@nus.edu.sg
* Correspondence: mpegm@nus.edu.sg; +65-6516-6358 (M.G.); mallick@iitism.ac.in (A.M)

Abstract: The present study investigated the effects of alloying and nano-reinforcement on the mechanical properties (microhardness, tensile strength, and compressive strength) of Mg-based alloys and composites. Pure Mg, Mg-3Sn alloy, and Mg-3Sn+0.2GNP alloy-nanocomposite were synthesized by powder metallurgy followed by hot extrusion. The microstructural characteristics of the bulk extruded samples were explored using X-ray diffraction, field-emission scanning electron microscopy, and optical microscopy and their mechanical properties were compared. The microhardness, tensile strength, and compressive strength of the Mg-3Sn alloy improved when compared to those of monolithic Mg sample and further improvements were displayed by Mg-3Sn+0.2GNP alloy-nanocomposite. No significant change in the compressive strain to failure was observed in both the alloy and the alloy-nanocomposite with respect to that of the pure Mg sample. However, an enhanced tensile strain to failure was displayed by both the alloy and the alloy-nanocomposite.

Keywords: Alloy; nanocomposite; magnesium; synthesis; microstructure; mechanical properties

1. Introduction

Magnesium is widely used as a high-performance structural material due to its low density, good hardness, and high specific strength [1–3]. The density ratios of magnesium alloys to aluminum and steel are approximately 2:3 and 1:4, respectively, which are comparable to those of plastic and carbon fiber composites. Magnesium also offers other potential properties, such as excellent castability, machinability, weldability, damping, and resistance to electromagnetic radiation [4, 5]. The melting temperature and specific strength of Mg are comparable to those of aluminum alloys [6]. Mg is the lightest structural metal and available in abundance in the earth's crust and seawater. Mg-based alloys and composites are considered as a replacement for heavier materials in manufacturing industries such as steels, titanium and aluminum alloys. The need for reducing the weight of automobile components after the introduction of the new legislation to low emission has triggered a renewed interest in Mg alloys [7]. Mg is also recognized as a potential candidate for medical implants due to its biocompatibility [8, 9]. Despite outstanding properties, the application of Mg alloys in critical engineering is limited. The Mg alloys of AZ and AM series are the most cost-effective ones among the available limited choices, however, they exhibit low strength and low creep resistance. Therefore, in order to fulfill industrial needs for wider applications, the development of novel magnesium alloys with better strength and creep resistance at lower costs is utmost necessary [10]. Tin (Sn) is a potential alloying element to develop Mg-Sn alloys. Mg-Sn alloys show better corrosion

 doi:10.20944/preprints202011.0660.v1

resistance than pure magnesium (Mg) and possess excellent mechanical properties and creep-resistance at high temperatures due to the presence of the Mg_2Sn phase. The melting point of this intermetallic phase in Mg-Sn alloys (770°C) is much higher than that of the $Mg_{17}Al_{12}$ phase in Mg-Al alloys (462°C) [11–13].

The addition of nanoparticles is another approach to improve the strength and ductility of Mg alloys. The addition of oxide nanoparticles (Al_2O_3, Y_2O_3, TiO_2, ZnO, ZrO_2, Sm_2O_3, and CeO_2), carbides (B_4C, SiC, and TiC), nitrides (TiN, BN, and AlN), borides (SiB_6, TiB_2, and ZrB_2), and CNTs can enhance the strength and ductility of Mg simultaneously [6]. The incorporation of thermally stable nanoparticles (ZnO, SiO_2, Sm_2O_3, and La_2O_3) can also improve the ignition properties of Mg. The incorporation of small percentage of SiO_2 and Sm_2O_3 nanoparticles can improve the ignition temperature of Mg by 69°C [14, 15]. The Mg-1.8Y/1CaO nanocomposite fabricated by Tekumalla et al. [16] displayed the onset of ignition at 1045°C. Graphene nanoplatelets (GNPs) exhibit superior mechanical, thermal, electrical, and tribological properties [17–20]. GNPs has the potential to significantly improve the performance of different metals (Mg, Al, Cu, Fe, Ni), alloys, and intermetallic compounds. Graphene-reinforced metal/alloy matrix composites manifest excellent mechanical, thermal, and electrical properties. In addition, GNPs can be produced on a large scale at a low cost. The proper dispersion of GNPs in the matrix is a crucial consideration to improve the performance of metal matric composites (MMCs). The agglomeration of GNPs due to the Vander-Waal force and the π-π stacking effect creates a significant challenge during the processing of composites. Different Mg-Sn alloys with improved mechanical properties and creep resistance have been fabricated by casting. However, conventional casting is not suitable to mix nanoparticles uniformly due to agglomeration issues. Powder metallurgy, melting and solidification, electrochemical deposition, thermal spraying, and other novel processing routes are generally used to fabricate graphene-based MMCs [21–24]. Rashad et al. [25] reported an improvement in the mechanical properties of pure Mg and Mg-1Al-1Sn alloy after the incorporation of a low amount of GNP (0.18–0.3 wt. %). Khurram Munir et al. [26] fabricated Mg-GNP MMCs with different graphene contents (0.1 wt.%, 0.2 wt.%, and 0.3 wt.%) and obtained positive results in terms of compression, corrosion, and biocompatibility. Kumar et al. [20] fabricated Mg-3Al/xGNP (x = 0.1 wt.%, 0.3 wt.%, and 0.5 wt.%) alloy-nanocomposites with improved mechanical and tribological properties.

The results of literature search indicates that no work is conducted so far in using GNP in aluminum free magnesium alloys. Accordingly, in the present study, pure Mg, Mg-3Sn alloy (in wt.%), and Mg-3Sn+0.2GNP alloy-nanocomposites (in wt.%) were fabricated through powder metallurgy followed by hot extrusion. The effects of GNP and alloying element tin on the microstructural and mechanical properties of magnesium were critically investigated.

2. Materials and Methods

2.1 Materials

Magnesium powder (60–300 μm) from Merck, Germany, tin powder (99.9% pure, 45 μm) from Goodfellow Cambridge Limited, Huntingdon, England, graphene nanoplatelets (thickness = 6–10 nm and width = 15 μm) from Tokyo Chemical Industry Co. Ltd., Japan were used as raw materials. The Mg:Sn ratio in the alloy was 97:3 (in wt%), and the Mg-Sn+GNP ratio in the alloy-nanocomposite was 97:3+0.2 (in wt.%).

2.2. Synthesis

Preprints (www.preprints.org) | NOT PEER-REVIEWED | Posted: 26 November 2020 doi:10.20944/preprints202011.0660.v1

Pure bulk Mg, Mg-3Sn alloy, and Mg-3Sn+0.2GNP alloy-nanocomposite were synthesized by powder metallurgy. Mg, Sn, and GNP powders were mixed at different ratios, and no process control agent was used during mixing. Except for pure Mg, a Turbula® T 2 F mixer (Make: Willy A. Bachofen AG, Switzerland) rotated at 50 rpm for one hour was used for the homogeneous mixing of Sn and GNPs. Rubber mold with an inner diameter of 50 mm was filled with the powder mixtures up to a height of 80 mm under continuous tapping. The rubber mold was then subjected to cold isostatic compression under a water pressure of 370 MPa. The green compacts were sintered in a box furnace at 500°C for two hours under an argon atmosphere. The sintered billets were then machined to a size of 35 mm (diameter) × 40 mm (height). The resultant machined billets were homogenized at 400°C for one hour and then hot extruded at 350°C. The extrusion ratio was set to 20.25:1 to produce 8 mm diameter rods.

2.3. X-ray Diffraction Analysis

The X-ray diffraction analysis of the extruded samples was performed in an automated Shimadzu LAB-XRD-6000 (Cu Kα; λ= 1.54 Å) spectrometer with a scan rate of 2^0/min. The phases present in the samples were analyzed from the intensities of X-ray diffraction peak.

2.4. Density and Porosity Measurement

The theoretical densities of the powder samples were obtained by the rule-of-mixture, and the experimental densities of the bulk samples were estimated by Archimedes' principle [27]. The bulk samples of each composition were weighed in air and water with the help of a weighing machine (Model: PRACTUM213–10IN, Germany; accuracy = 0.0001 g). The theoretical densities of Mg, Sn, and GNP were considered as 1.74 g.cm^{-3}, 7.28 g.cm^{-3}, and 2.30 g.cm^{-3}, respectively.

2.5. Microhardness Test

The microhardness values of the samples were measured by an MTR3/50–50/NI machine equipped with Tribotester software. The samples were cut from the middle portion of the extruded rods and then made flat and polished to perform indentation tests. A load of 5 N was applied by an indenter with a loading rate of 5 N/min followed a dwell period of 30 s. A Vickers pyramidal diamond indenter with a phase angle of 136° was used for indentation tests. Five indentations at different places were made for each sample to avoid discrepancies in the obtained results.

2.6. Microstructural Characterization

The field-emission scanning electron microscopy (FESEM) images of GNPs, the elemental area mapping of different samples, the identification of the Mg_2Sn phase in the composite, and the morphologies of fracture surfaces after tensile and compressive tests were obtained using Carl Zeiss Supra FESEM.

2.7. Tensile Test

Tensile tests of the extruded samples were performed on a Tinius Olsen (H50KS) mechanical testing machine with a strain rate of 1.6×10^{-4} s^{-1}. Dog-bone-shaped tensile specimens with a gauge diameter of 4 mm and a gauge length of 20 mm were prepared from 8 mm extruded rods according to the ASTM E8/E8M-13a standard. The samples were machined using a CNC lathe machine and

 doi:10.20944/preprints202011.0660.v1

then polished to remove uneven surfaces. A minimum of three tests were performed for each sample to ensure reliability of the results.

2.8. Compression Test

Compression tests were performed on a Hounsfield mechanical testing machine (H50KS) according to the ASTM E9–09 standard. The tests were carried out on the extruded cylindrical samples of 7 mm diameter and 7 mm length. The strain rate was set to 8.3×10^{-5} s^{-1}. Five tests were conducted for each sample to ensure the consistency of the results..

3. Results and discussion

3.1. Density measurement anlysis

Pure bulk Mg, Mg-3Sn alloy, and Mg-3Sn+0.2GNP alloy-nanocomposite were successfully synthesized using powder metallurgy technique followed by hot extrusion. The densities and porosities of the bulk extruded samples of three compositions are reported in Table 1. Almost negligible amount of variation between the theoretical and experiment densities were observed. These results suggest the extruded samples were nearly dense. The alloy and composites samples exhibited less porosity as compared to pure Mg sample. This result attributed good interfacial bonding between the matrix and the nano-reinforcement.

Table 1. Density (g/cc) measurements of pure Mg, alloy and nanocomposite

Material	Theoretical density	Experimental density	Porosity (%)
Mg	1.740	1.707 ±0.0040	1.90
Mg-3Sn	1.781	1.766 ±0.0028	0.84
Mg-3Sn+0.2GNP	1.782	1.765 ±0.0017	0.95

3.2 XRD anlysis

Figure 1 presents the X-ray diffraction line profile of the extruded samples of pure Mg, Mg-3Sn alloy and Mg-3Sn+0.2GNP alloy-nanocomposite. The results reveal that the α-Mg phase was present in both the Mg-3Sn alloy and the Mg-3Sn+0.2GNP alloy-nanocomposite. The absence of the Sn peak indicates the formation of a solid solution of pure Mg and Sn. Due to the addition of a very small amount of GNPs in the Mg matrix, the peak intensities of GNPs were almost invisible. A similar observation was reported by Chen et al. [4]. Some of the peaks of Mg_2Sn with lower intensities were observed in the XRD pattern.

Preprints (www.preprints.org) | NOT PEER-REVIEWED | Posted: 26 November 2020 doi:10.20944/preprints202011.0660.v1

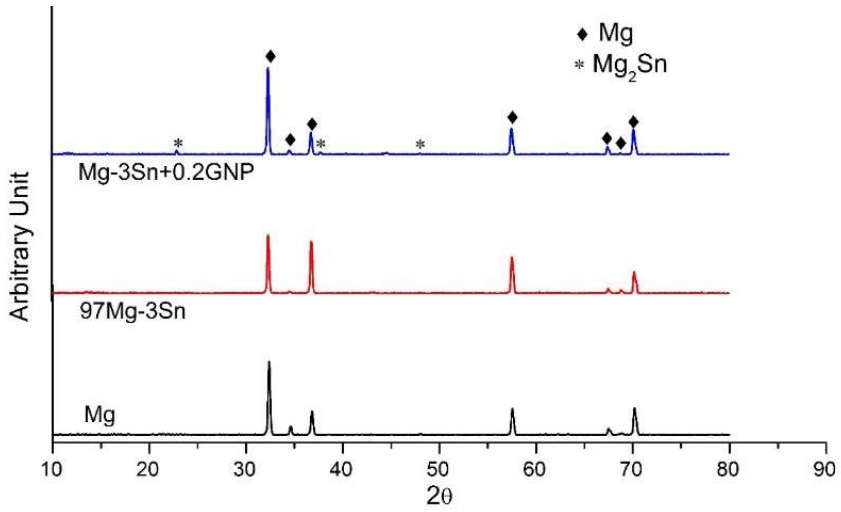

Figure 2. XRD results of extruded samples of pure Mg, Mg-3Sn alloy and Mg-3Sn+0.2GNP nanocomposite.

3.3 Microstructural anlysis

Figure 2 represents the FESEM image of the graphene nanoplate. It could be seen that the graphene sheets are exfoliated that resembles a loose sponge like structure. The ultrathin crumpled layer platelets are visible to the electron beam. The presence of the polygonal and lathe-shaped Mg_2Sn phase in the Mg-3Sn+0.2GNP nanocomposite was confirmed by FESEM (Figure 3) [28, 29] image analysis. The FESEM-EDX elemental area mapping in Figure 4 reveals that a small cluster of GNPs was evenly distributed in the alloy matrix and acted as a grain nucleation agent to pin the grain boundary.

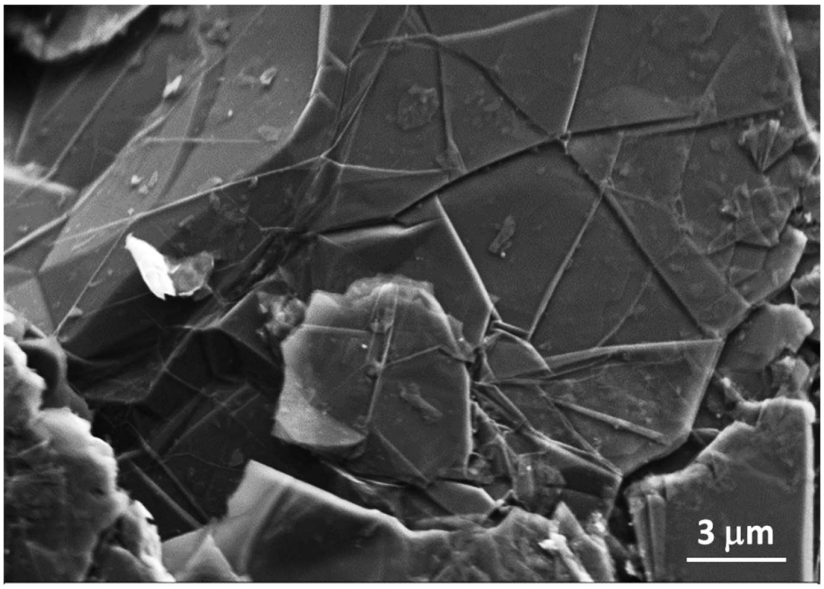

Figure 1. FESEM image of graphene nanoplatelets.

Preprints (www.preprints.org) | NOT PEER-REVIEWED | Posted: 26 November 2020 doi:10.20944/preprints202011.0660.v1

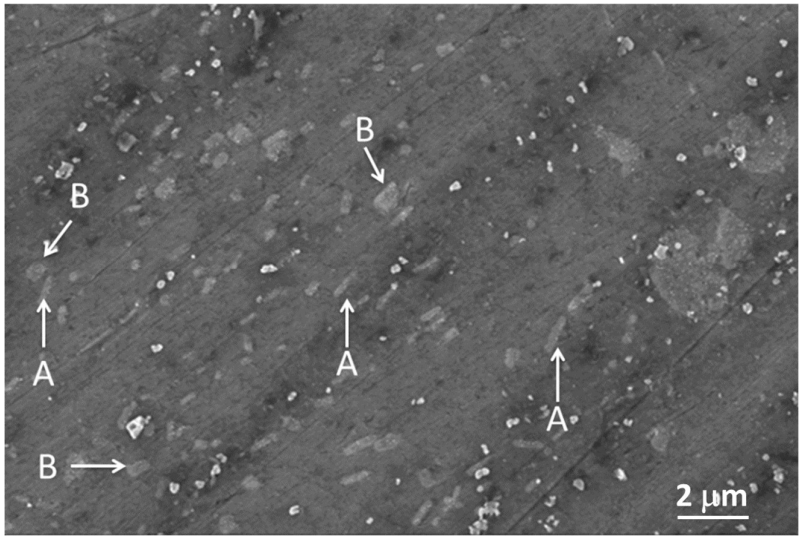

Figure 3. FESEM morphology of Mg_2Sn phase in the form of lathe/rod (A) and polygon (B) in the Mg-3Sn+0.2GNP alloy-nanocomposite

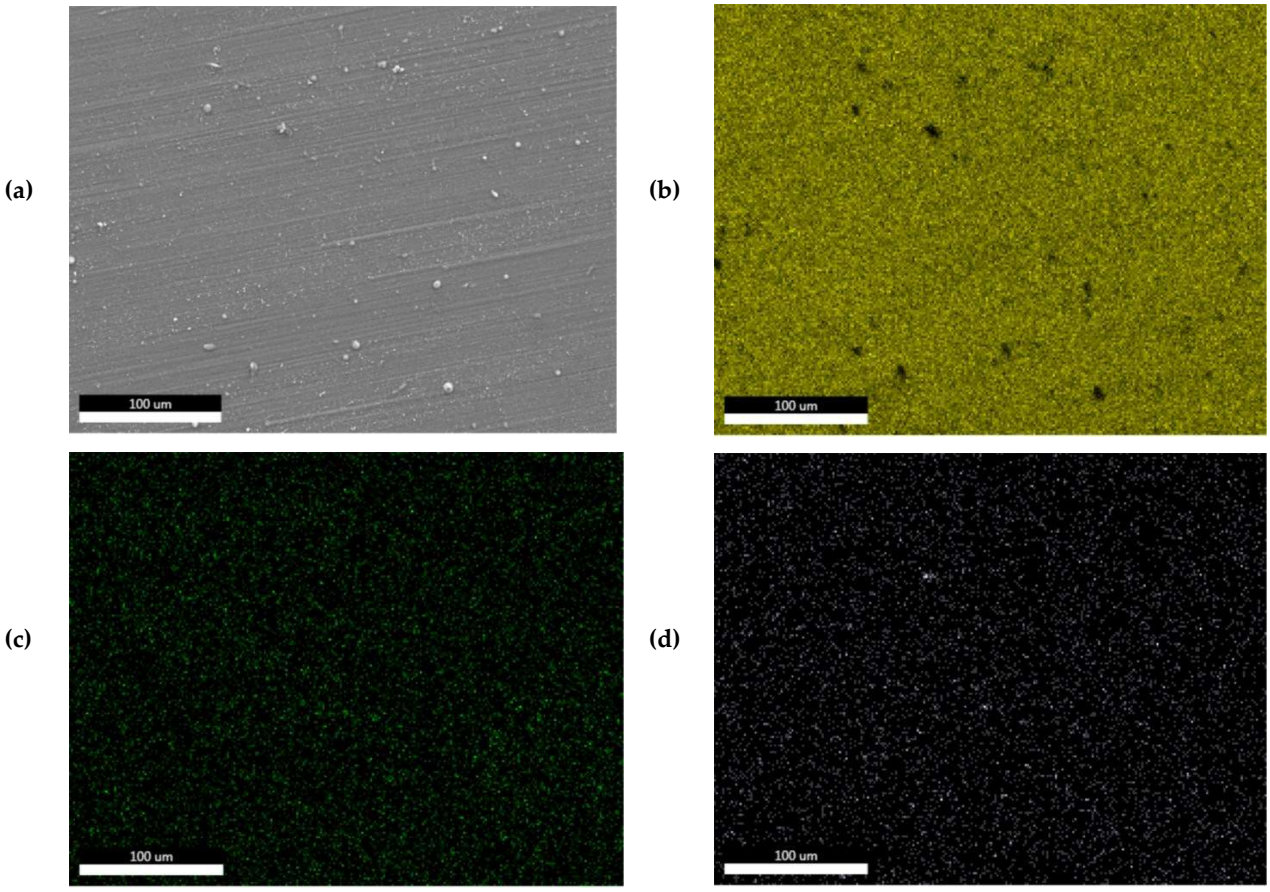

Figure 4. FESEM-EDX elemental area mapping of the Mg-3Sn+0.2GNP nanocomposite: (a) FESEM image of a selected area, (b) Mg, (c) Sn, and (d) Carbon (GNP).

Preprints (www.preprints.org) | NOT PEER-REVIEWED | Posted: 26 November 2020 doi:10.20944/preprints202011.0660.v1

3.4 Microhardness and Tenstile properties

Table 2 presents the Vickers microhardness values and tensile properties of the three samples. It can be seen that after the addition of Sn and GNP, the room-temperature mechanical properties of the Mg-3Sn-0.2GNP nanocomposite were invariably improved. The microhardness of the Mg-3Sn+0.2GNP alloy-nanocomposite was improved by 7.8% and 22.4% with respect to those of the Mg-3Sn alloy and pure Mg, respectively. The microhardness of the Mg-3Sn alloy was ~32% higher than that of pure Mg. It happened because the alloying element Sn formed the Mg_2Sn phase, which is more thermally and mechanically stable and contributed to precipitation hardening and dispersion hardening. Further addition of the harder reinforcement (GNP) caused dispersion hardening and hindered dislocation mobility through the suppression of recrystallization and crystal grain growth [30].

Table 2. Micro-hardness and tensile properties at room temperature.

Material	Vicker's hardness (HV)	0.2% Offset yield strength (Nmm^{-2})	Ultimate tensile strength (Nmm^{-2})	Failure strain (%)
Mg	38 ±4	82 ±3	151 ±3	17.9 ±0.7
Mg-3Sn	50 ±4	132 ±11	185 ±10	21.3 ±2.2
Mg-3Sn+0.2GNP	54 ±3	136 ±21	201 ±7	21.8 ±1.6

Figure 5 displays the tensile engineering stress-strain curves of the three samples at room temperature. The ultimate tensile strength of the alloy-nanocomposite was 8.8% and 33.5% greater than those of the alloy and pure Mg, respectively.

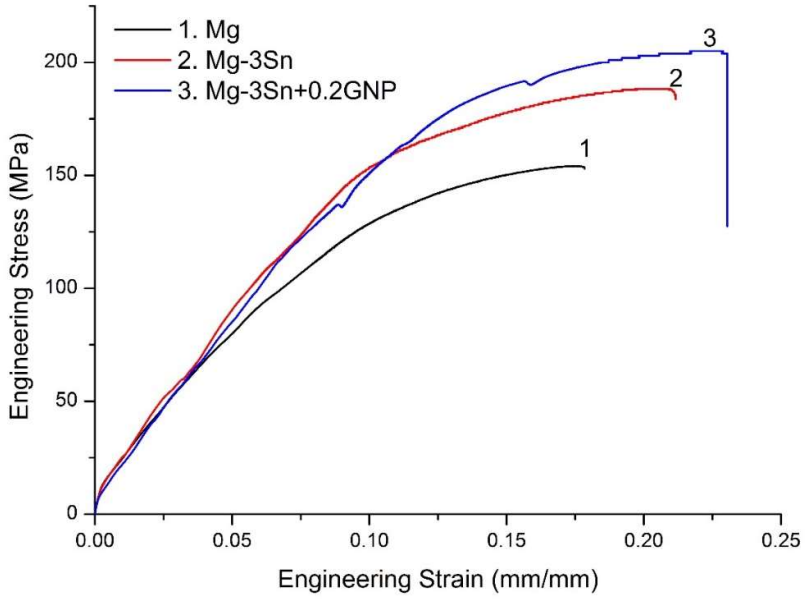

Figure 5. Representative tensile engineering stress-strain curve.

The Zener pinning by GNP reinforcement induced microstructural refinement contributed to the simultaneous enhancement of strength and hardness [31]. The strengthening of the Mg-3Sn matrix was associated with the load transfer from the Mg matrix to Mg_2Sn and GNPs, the increased dislocation density due to thermal expansion coefficient (CTE) mismatch and elastic modulus

Preprints (www.preprints.org) | NOT PEER-REVIEWED | Posted: 26 November 2020 doi:10.20944/preprints202011.0660.v1

mismatch, Orowan looping, and solid solution strengthening [32]. The prismatic punching of dislocation at the interface of the alloy matrix and GNP nanoparticles resulted in work hardening due to the CTE mismatch. The CTE mismatch between the Mg-3Sn alloy matrix and GNPs promoted the wrinkling effect in GNPs and further hindered dislocation movements [33]. The elastic modulus mismatch between the alloy matrix and GNPs generated dislocations due to inhomogeneous slips. Saba et al. [34] reported that the elastic modulus difference between the matrix and reinforcement particles improved the strength of the composite during work hardening by enhancing interfacial bonding. The Mg_2Sn phase in the Mg-3Sn alloy and GNPs in the Mg-3Sn-0.2GNP alloy-nanocomposite acted as obstacles and improved the strength by Orowan looping. Residual dislocation loops were formed around precipitates after dislocations bowed out and bypassed them, resulting in a higher work hardening effect under the applied load. The ductility of the Mg-3Sn alloy was higher than that of pure Mg, and the further addition of 0.2 wt.% GNP improved the ductility of Mg-3Sn+0.2GNP. The failure strain of Mg-3Sn+0.2GNP was enhanced by 2.3% and 21.8% with respect to those of the Mg-3Sn alloy and pure Mg, respectively. Fig. 6 presents the fracture surface morphologies of the tensile samples. The fracture surface morphology of pure Mg featured brittle failure due to a limited number of slip systems clearly showing microscopically small rough cleavages and steps. The fracture surface morphology of Mg-3Sn and Mg-3Sn+0.2GNP featured ductile failure as dimples and tear ridges were formed on the surface through a void-sheet mechanism. Intergranular crack propagation was also noticed in the alloy.

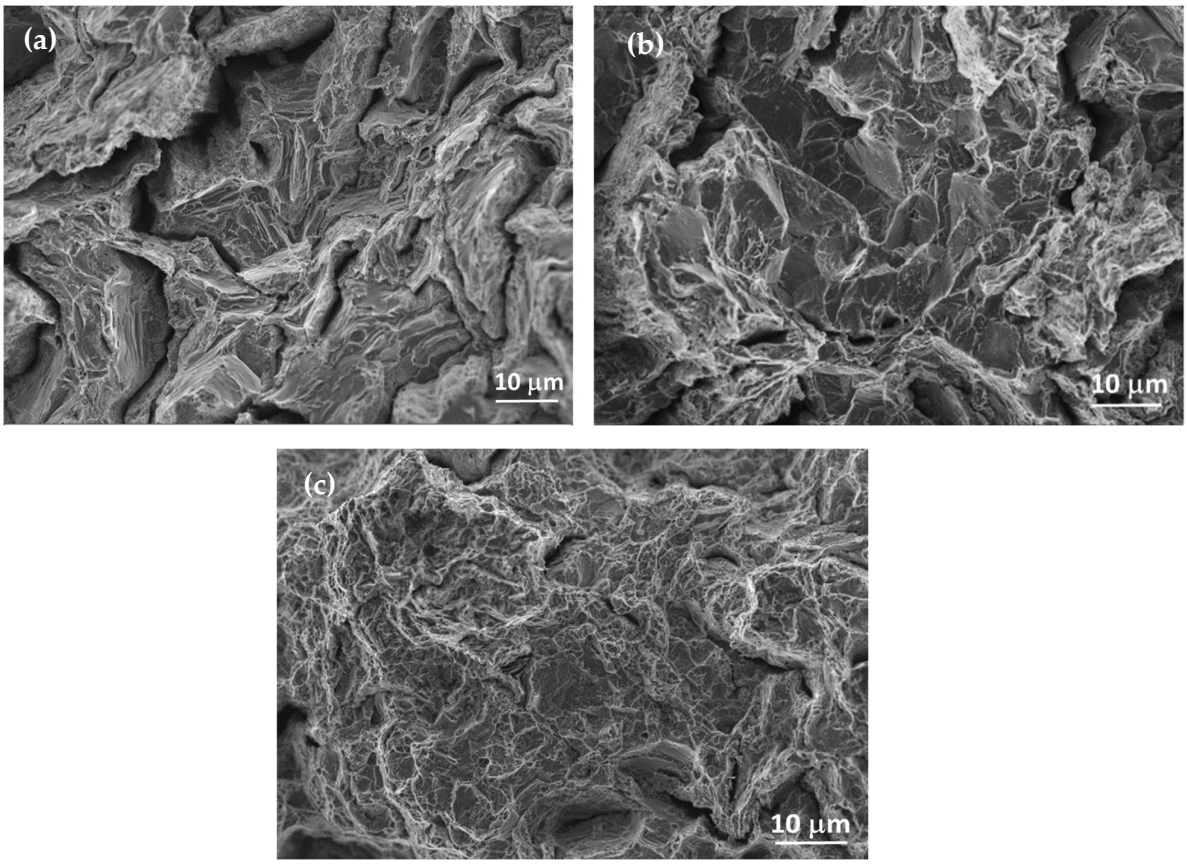

Figure 6. Fracture surface morphology of tensile failure samples: (a) Mg, (b) Mg-3Sn and (c) Mg-3Sn+0.2GNP

Preprints (www.preprints.org) | NOT PEER-REVIEWED | Posted: 26 November 2020 doi:10.20944/preprints202011.0660.v1

3.5. Compressive Properties

Table 3 presents the room-temperature compressive properties of all three compositions. Figure 7 shows the behavior of engineering compressive stress-strain curves at room temperature. The compressive strength of Mg-3Sn+0.2GNP was improved by 10.7% and 32.9% with respect to the Mg-3Sn alloy and pure Mg, respectively without compromising the failure strain. Fig. 8 presents the surface fracture morphologies of the compressed samples. The presence of a shear band on the fracture surfaces of all samples indicates shear failure. The fracture surface in the Mg-3Sn+0.2GNP composite was observed to be smooth and the presence of less micro crack as compare to pure Mg and alloy. An improvement in compressive ductility was noticed after the addition of nano-GNPs [35, 36]. An activation of non-basal slip through grain refinement occurred after the addition of GNPs in the alloy matrix. The activation of non-basal slip could improve the deformation behavior under tensile loading by weakening the basal texture, which is preferentially aligned in hot-extruded Mg materials along the extrusion direction [37]. The deformation of Mg-based materials under compressive loading along the extrusion direction occurs through twinning, followed by slip [38]. Under compressive loading, failure strain is normally reduced due to the presence of the second phase, which hinder the twinning process. No significant change in failure strain occurred due to the compensating effect of Mg_2Sn and GNPs was observed in the present study.

Table 3 Compressive properties at room temperature

Material	0.2% Offset yield strength (Nmm^{-2})	Ultimate compressive strength (Nmm^{-2})	Failure strain (%)
Mg	115 ±8	341 ±11	23.3 ±0.8
Mg-3Sn	138 ±14	409 ±24	24.6 ±1.5
Mg-3Sn-0.2GNP	159 ±9	453 ±19	25 ±1.1

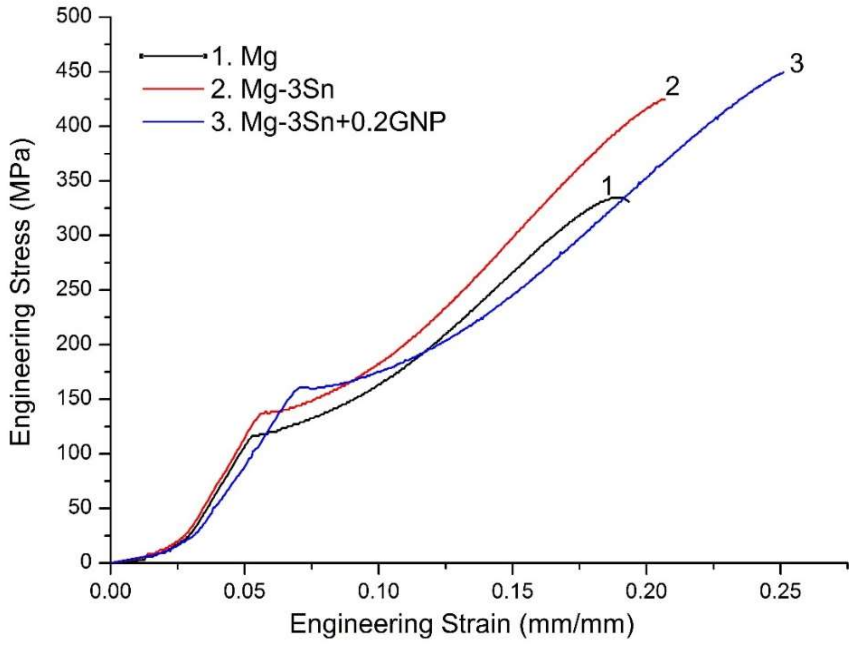

Figure 7. Representative compressive engineering stress-strain curves.

Preprints (www.preprints.org) | NOT PEER-REVIEWED | Posted: 26 November 2020 doi:10.20944/preprints202011.0660.v1

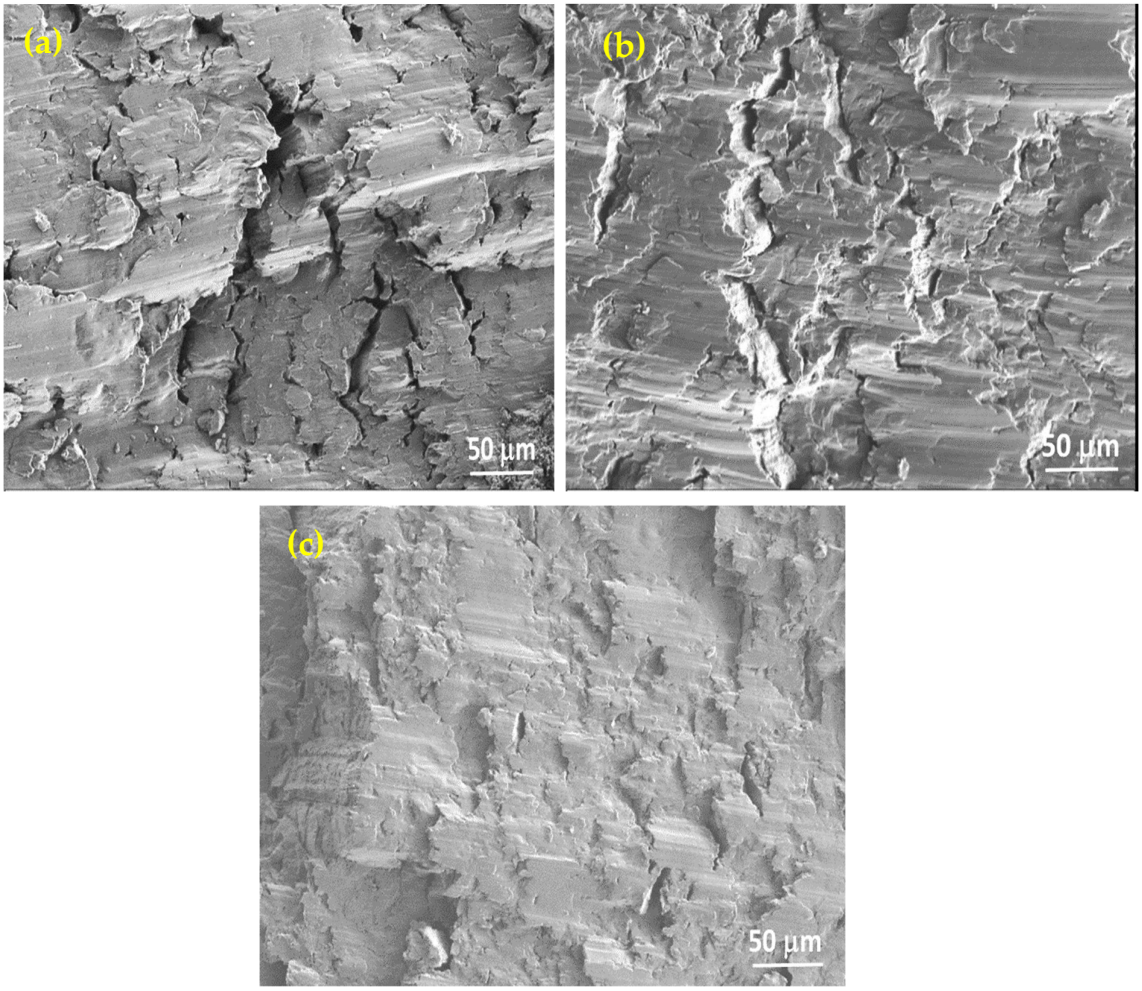

Figure 8. Fracture surface morphology of compressive failure samples: (a) Mg, (b) Mg-3Sn, and (c) Mg-3Sn+0.2GNP.

4. Conclusions

Pure bulk Mg, Mg-3Sn alloy, and Mg-3Sn+0.2GNP alloy-nanocomposite were fabricated by powder metallurgy assisted by sintering in an inert atmosphere. The effects of Sn and GNP addition on mechanical and microstructural properties were studied. The main observations are presented below.

1. The microhardness of the Mg-3Sn alloy was improved by 22.4% with respect to that of pure Mg. The microhardness of the Mg-3Sn+0.2GNP was improved by 42.4% and 7.8% with respect to those of pure Mg and the Mg-3Sn alloy, respectively.
2. The ultimate tensile strength of the Mg-3Sn alloy was improved by 22.5% with respect to that of pure Mg. The ultimate tensile strength of Mg-3Sn+0.2GNP was improved by 33.5% and 9% with respect to those of pure Mg and the Mg-3Sn alloy, respectively.
3. The ultimate compressive strength of the Mg-3Sn alloy was improved by 20% with respect to that of pure Mg. The ultimate compressive strength of Mg-3Sn+0.2GNP was improved by 32.9% and 10.7% with respect to those of pure Mg and the Mg-3Sn alloy, respectively.

4. After the addition of 0.2% GNP in the Mg-3Sn alloy, the improvement in the tensile strength (+16.6 MPa) of the Mg-3Sn+0.2GNP alloy-nanocomposite was lower than that of the compressive strength (+43.7 MPa).

.

Funding: This research received no external funding.

Acknowledgments: The authors gratefully acknowledge the Department of Science & Technology, Government of India (project no.: SB/EMEQ-020/2013) for providing materials and MTR3/50-50/NI machine (MICROTEST S. A., Spain) in which hardness tests were performed.

Conflicts of Interest: The authors declared that there is no potential conflict of interest with respect to the research, authorship, and publication of this paper.

References

1. Kainer, K. U.; ed. *Magnesium alloys and technology*. John Wiley & Sons, 2003.
2. Xu, W. et al. A high-specific-strength and corrosion-resistant magnesium alloy. *Nature Materials* **2015**, 14, 1229-1235.
3. Mallick, A.; Vedantam, S.; Li, L. Grain size dependent tensile behavior of Mg–3% Al alloy at elevated temperatures. *Mater. Sci. Eng. A* **2009**, 515, 14-18.
4. Zhang, X.; Lihua, L.; Naiheng, M.; Haowei, W. Mechanical properties and damping capacity of magnesium matrix composites. *Composites Part A: Applied Science and Manufacturing* **2006**, 37, 2011-2016.
5. Manakari, V.; Parande, G.; Gupta, M. Selective laser melting of magnesium and magnesium alloy powders: a review. *Metals* **2017**, 7, 2.
6. Wong, W. L. E.; Gupta, M. High performance lightweight magnesium nano composites for engineering and biomedical applications. *Nano World Journal* **2016**, 2, 78-83.
7. Ferguson, J. B.; Jaberi, F.S.; Kim, C.S., Rohatgi, P.K.; Cho, K. On the strength and strain to failure in particle-reinforced magnesium metal-matrix nanocomposites (Mg MMNCs). *Mater. Sci. Eng. A* **2012**, 558, 193-204.
8. Kraus, T.; Fischerauer, S.F.; Hanzi, A.C.; Uggowitzer, P.J.; Loffler, J.F.; Weinberg, A.M. Magnesium alloys for temporary implants in osteosynthesis: in vivo studies of their degradation and interaction with bone. *Acta biomaterialia* **2012**, 8, 1230-1238.
9. Kirkland, N.T.; Birbilis, N. *Magnesium biomaterials: design, testing, and best practice*. Springer International Publishing, 2014.
10. Seetharaman, S.; et al. Effect of erbium modification on the microstructure, mechanical and corrosion characteristics of binary Mg–Al alloys. *J. of Alloys and Compounds* **2015**, 648, 759-770.
11. Chen, J.H.; Shen, Y.C.; Chao, C.G.; Liu, T.F. Wear Behavior and Microstructure of Mg-Sn Alloy Processed by Equal Channel Angular Extrusion. *Materials* **2017**, 10, 1315.
12. Ha, H.Y.; Kang, J.Y.; Yang, J.; Yim, C.D.; You, B.S. Role of Sn in corrosion and passive behavior of extruded Mg-5 wt% Sn alloy. *Corrosion Science* **2016**, 102, 355-362.
13. Liu, H.; Chen, Y.; Tang, T.; Wei, S.; Niu, G. The microstructure, tensile properties, and creep behavior of as-cast Mg–(1–10)% Sn alloys. *J. of Alloys and Compounds* **2007**, 440, 122-126.
14. Parande, G.; Manakari, V.; Meenashisundaram, G.K.; Gupta, M. Enhancing the tensile and ignition response of monolithic magnesium by reinforcing with silica nanoparticulates. *J. Mater. Res.* **2017**, 32, 2169-2178.
15. Kujur, M.S.; Mallick, A.; Manakari, V.; Parande, G.; Tun, K.S.; Gupta, M. Significantly enhancing the ignition/compression/damping response of monolithic magnesium by addition of Sm_2O_3 nanoparticles. *Metals* **2017**, 7, 357.
16. Tekumalla, S.; Nandigam, Y.; Bibhanshu, N.; Rajashekara, S.; Yang, C.; Satyam, S.; Gupta, M. A strong and deformable in-situ magnesium nanocomposite igniting above 1000 C." *Scientific reports* **2018**, 8, 1-10.
17. Moghadam, A.D.; Omrani, E.; Menezes, P.L.; Rohatgi, P.K. Mechanical and tribological properties of self-lubricating metal matrix nanocomposites reinforced by carbon nanotubes (CNTs) and graphene–a review. *Composites Part B: Engineering* **2015**, 77, 402-420.
18. Papageorgiou, D.G.; Kinloch, I.A.; Young, R.J. Mechanical properties of graphene and graphene-based nanocomposites. *Progress in Materials Science* **2017**, 90, 75-127.
19. Novoselov, K.S.; Falko, V.I.; Colombo, L.; Gellert, P.R.; Schwab, M.G.; Kim, K. A roadmap for graphene. *Nature* **2012**, 490, 192-200.

20. Kumar, P.; Mallick, A.; Kujur, M.S.; Tun, K.S.; Gupta, M. Effects of graphene nanoplatelets on the tribological, mechanical, and thermal properties of Mg-3Al alloy nanocomposites. *Int. J. of Mat. Res.* **2019**, 110, 534-542.
21. Hu, Z.; Tong, G.; Lin, D.; Chen, C.; Guo, H.; Xu, J.; Zhou, L. Graphene-reinforced metal matrix nanocomposites–a review. *Materials Science and Technology* **2016**, 32, 930-953.
22. Xiang, S.; Wang, X.; Gupta, M.; Wu, K.; Hu, X.; Zheng, M. Graphene nanoplatelets induced heterogeneous bimodal structural magnesium matrix composites with enhanced mechanical properties. *Scientific reports* **2016**, 6, 38824.
23. Rashad, M.; Pan, F.; Hu, H.; Asif, M.; Hussain, S.; She, J. Enhanced tensile properties of magnesium composites reinforced with graphene nanoplatelets. *Mater. Sci. Eng. A* **2015**, 630, 36-44.
24. Kumar, P.; Mallick, A.; Kujur, M.S.; Tun, K.S.; Shabadi, R.; Gupta, M. Strength of Mg–3% Al alloy in presence of graphene nano-platelets as reinforcement. *Materials Science and Technology* **2018**, 34, 1086-1095.
25. Rashad, M.; Pan, F.; Asif, M.; Tang, A. Powder metallurgy of Mg–1% Al–1% Sn alloy reinforced with low content of graphene nanoplatelets (GNPs). *journal of Industrial and Engineering Chemistry* **2014**, 20, 4250-4255.
26. Munir, K.; Wen, C.; Li, Y. Graphene nanoplatelets-reinforced magnesium metal matrix nanocomposites with superior mechanical and corrosion performance for biomedical applications. *Journal of Magnesium and Alloys* **2020**, 8, 269-290.
27. Ratcliffe, R.T. The measurement of small density changes in solids. *British Journal of Applied Physics* **1965**, 16, 1193.
28. Thenambika, V.; Jayalakshmi, S.; Singh, A.; Nidhi, J.K. Impression creep behaviour of extruded Mg-Sn alloy. *Int. J. of Vehicle Structures & Systems* **2016**, 8, 174-178.
29. Pekguleryuz, M.O.; Kainer, K.U.; Kaya, A.A. *Fundamentals of magnesium alloy metallurgy*. Woodhead Publishing Ltd., 2013.
30. Gupta, M.; Sharon, N.M.L. *Magnesium, magnesium alloys, and magnesium composites*. John Wiley & Sons, 2011.
31. Johanes, M.; Tekumalla, S.; Gupta, M. Fe_3O_4 nanoparticle-reinforced magnesium nanocomposites processed via disintegrated melt deposition and turning-induced deformation techniques. *Metals* **2019**, 9, 1225.
32. Ceschini, L.; Dahle, A.; Gupta, M.; et al. *Aluminum and magnesium metal matrix nanocomposites*. Springer, 2017.
33. Ogurtani, T.O; Dogukan, S.; Buke, G.C. Wrinkling of graphene because of the thermal expansion mismatch between graphene and copper. *Surface and Interface Analysis* **2018**, 50, 547-551.
34. Saba, F., Zhang, F.; Liu, S., Lie, T. Reinforcement size dependence of mechanical properties and strengthening mechanisms in diamond reinforced titanium metal matrix composites. *Composites Part B: Engineering* **2019**, 167, 7-19.
35. Tun, Khin Sandar. *Development and characterization of new magnesium based nanocomposites*. PhD. Thesis, National University of Singapore, Singapore, 2009.
36. Dieringa, H. Properties of magnesium alloys reinforced with nanoparticles and carbon nanotubes: a review. *J. of Materials Science* **2011**, 46, 289-306.
37. Sankaranarayanan, S.; Nayak, U.P.; Sabat, R.K.; Suwas, S.; Almajid, A.; Gupta, M. Nano-ZnO particle addition to monolithic magnesium for enhanced tensile and compressive response. *J. of alloys and compounds* **2014**, 615, 211-219.

 doi:10.20944/preprints202011.0660.v1

38. Kujur, M.S.; Manakari, V.; Parande, G.; Tun, K.S.; Mallick, A.; Gupta, M. Enhancement of thermal, mechanical, ignition and damping response of magnesium using nano-ceria particles. *Ceramics International* **2018**, 44, 15035-15043.